Available online at www.sciencedirect.com

ScienceDirect

Neuromuscular Disorders 27 (2017) 836–842

www.elsevier.com/locate/nmd

Insights from genotype–phenotype correlations by novel *SPEG* mutations causing centronuclear myopathy

Haicui Wang [a,b,1], Claudia Castiglioni [c,1], Ayşe Kaçar Bayram [d,1], Fabiana Fattori [e], Serdar Pekuz [a,b], Diego Araneda [f], Hüseyin Per [d], Ricardo Erazo [g], Hakan Gümüş [d], Suzan Zorludemir [h], Kerstin Becker [a,b], Ximena Ortega [f], Jorge Alfredo Bevilacqua [i,j], Enrico Bertini [e], Sebahattin Cirak [a,b,*]

[a] *Department of Pediatrics, University Hospital Cologne, Kerpener Str. 62, 50931 Cologne, Germany*
[b] *Center for Molecular Medicine Cologne (CMMC), University of Cologne, Robert-Koch-Str. 21, 50931 Cologne, Germany*
[c] *Unit of Neurology, Department of Pediatrics, Clinica Las Condes, Santiago, Chile*
[d] *Division of Pediatric Neurology, Department of Pediatrics, School of Medicine, Erciyes University, Kayseri, Turkey*
[e] *Unit of Neuromuscular and Neurodegenerative Disorders, Laboratory of Molecular Medicine, Bambino Gesu' Children's Hospital IRCCS, Rome, Italy*
[f] *Diagnostic Imaging Service, Clinica Las Condes, Santiago, Chile*
[g] *Neurology Unit, Hospital Luis Calvo Mackenna, Santiago, Chile*
[h] *Department of Pathology, School of Medicine, Çukurova University, Adana, Turkey*
[i] *Departamento de Neurología y Neurocirugía, Hospital Clínico Universidad de Chile, Santiago, Chile*
[j] *e Instituto de Ciencias Biomédicas, Facultad de Medicina, Universidad de Chile, Santiago, Chile*

Received 26 January 2017; received in revised form 8 May 2017; accepted 22 May 2017

Abstract

Centronuclear myopathies (CNM) are a clinically and genetically heterogeneous group of congenital myopathies, defined histologically by increased number of fibres with centrally located nuclei, and type I fibre predominance in muscle biopsy. Myotubular myopathy, the X-linked form of CNM caused by mutations in the phosphoinositide phosphatase MTM1, is histologically characteristic since muscle fibres resemble myotubes.

Here we present two unrelated patients with CNM and typical myotubular fibres in the muscle biopsy caused by mutations in *striated muscle preferentially expressed protein kinase (SPEG)*. Next generation sequencing revealed novel biallelic homozygous mutations in *SPEG* in both cases. Patient 1 showed the c.1627_1628insA (p.Thr544Aspfs*48) mutation and patient 2 the c.9586C>T (p.Arg3196*) mutation. The clinical phenotype was distinctive in the two patients since patient 2 developed a dilated cardiomyopathy with milder myopathy features, while patient 1 showed only myopathic features without cardiac involvement. These findings expand the genotype–phenotype correlations after the initial report. Additionally, we describe whole body muscle MRI of patient 2 and we argue on the different SPEG isoforms in skeletal muscle and heart as the possible explanation leading to variable phenotypes of *SPEG* mutations.

Keywords: *SPEG*; Exome; Centronuclear myopathy; Myotubular myopathy; Whole body MRI

1. Introduction

Congenital myopathies (CM) are a heterogeneous group of primary muscle diseases, most commonly manifesting with symptoms at birth, infancy or within the first two years of life. Severe muscle weakness is the major problem for patients with CM [1]. The severity of the clinical presentation can vary according to disease subtype from mild hypotonia causing delay of developmental motor milestones, usually noticed by the child's parents, to fatal forms due to cardiac and respiratory involvement in the neonatal period [1]. Centronuclear myopathies (CNM) are a subgroup of CM's, defined histologically by an increased number of fibers with central nuclei and type I fibre predominance [1]. Dynamin 2 related myopathy is defined by type I hypotrophy and radiated strands in the muscle biopsy [2]. CNM comprise a clinical spectrum of disorders that are classified by mode of inheritance, age of onset, differential

* Corresponding author. Department of Pediatrics, University Hospital Cologne, Kerpener Straße 62, 50937 Köln, Germany. Fax: +49 221 478 5189.
E-mail address: sebahattin.cirak@uk-koeln.de (S. Cirak).
[1] These authors contributed equally to this work.

http://dx.doi.org/10.1016/j.nmd.2017.05.014
0960-8966/

involvement of the affectedmuscles, disease course, and depending on the mutations of the involved genes [1]. Currently, mutations in CNM-causing genes have been identified for about 60–80% of the cases of centronuclear myopathy: Recessive X-linked mutations in *myotubularin 1* (*MTM1*, OMIM #300415), autosomal-dominant mutations in *dynamin 2* (*DNM2*, OMIM#602378) and *bridging integrator 1* (*BIN1*, OMIM#601248), autosomal recessive mutations in *BIN1*, *ryanodine receptor 1* (*RYR1*, OMIM#180901) and also in *titin* (*TTN,* OMIM#188840) [2–5].

In a recent report, mutations on the *striated muscle preferentially expressed protein kinase (SPEG)*, which interacts with MTM1 in myofibres, were demonstrated to cause CNM [6].

Following the initial report of Agrawal et al. [6], here we now report on two additional patients affected by CNM caused by two novel *SPEG* mutations, along with a complete description of the associated clinical, pathological and imaging findings. We also discuss about the genotype–phenotype correlations, and review the underlying molecular mechanism of SPEG as an interacting partner of MTM1 in excitation contraction coupling [6] in skeletal muscle and its role in the myocardium [7].

2. Materials and methods

2.1. Histopathology studies

The muscle biopsies of both patients were snap frozen in isopentane previously cooled in liquid nitrogen. Frozen sections were processed according to standard histological, histochemical and immunohistochemical techniques [8] (further details in the Supplementary material).

2.2. Whole body MRI

The institutional ethical board approved the study and informed consent was obtained from caregivers. Whole body-MRI images were acquired by a 1.5-Tesla Avanto Siemens MRI system, which was equipped with 2 BodyArray and 1 lower extremities surface coil. The patient was examined from head to toe in supine position with his arms beside the body in a lateral position (further details in the Supplementary material).

2.3. Genetics

The institutional ethical board approved the studies and informed consents were obtained from parents. For patient 1 genomic DNA isolated from EDTA-blood was sequenced for the Mendeliome gene panel as described earlier [9] (further details in the Supplementary material).

For Patient 2 genomic DNA isolated from EDTA-blood was used for the Nextera Rapid Capture Custom Enrichment Kit (Illumina, San Diego, California, USA), which was designed to target exons of 73 myopathy-related-genes, including the 6 genes related to CNM and the C-terminal domain of TTN. DNA capture, enrichment and paired-end sequencing with read length of 151 bp were performed using an Illumina MiSeq according to manufacturer's instructions and aiming for an average sequencing depth of 100-fold (further details in the Supplementary material). The Illumina VariantStudio data analysis software was used to annotate the variants.

3. Results

3.1. Clinical description

Patient 1 is a 3-year-old boy with hypotonia and motor developmental delay. His prenatal history and intrauterine ultrasonography follow-up were normal. He is the offspring of a non-consanguineous couple from the same Turkish village. He was delivered by caesarean section due to foetal bradycardia, as a 3050 g full-term neonate. No abnormalities were observed in his first post-natal examination. At 5 days of life, he presented apnoea, poor sucking and high-pitched cry, and was admitted to intensive care requiring incubation with oxygen insufflation. As the patient presented hypersomnolence and a hypotonic syndrome, a complete neurological assessment was performed. Cranial ultrasound and brain MRI revealed no abnormalities. Laboratory investigations including creatine kinase (CK), thyroid function tests, serum electrolytes, vitamin B12, ammonia, pyruvate, lactate, serum and cerebrospinal fluid (CSF) glycine levels were all in normal range. Inspiratory stridor was diagnosed to be associated with laryngomalacia in the first month of life. An echocardiography performed at 3 months of age was normal. Electrophysiological assessment was performed twice; the first assessment was reported to be normal, but the second revealed a myopathic pattern on needle EMG with fibrillations and polyphasic motor unit potentials, with normal motor and sensory nerve conduction studies in upper and lower limbs. A centronuclear myopathy with typical small fibres and central nuclei was detected in the muscle biopsy from the left thigh at the age of 13 months (Fig. 2a–c).

He developed recurrent pulmonary infections in the first 2 years of life. Head control was achieved at 6 months and unsupported sitting at 12 months of age, but he never achieved independent walking. On the latest examination at the age of 34 months, his weight and head circumference were below the 3rd percentile, while the height was in the 86th percentile respectively. He had a high arched palate and *pes cavus* (Fig. 1a, b). He showed interest in the environment, showed passive understanding, knew a few words but was unable to speak even two sentences just single words. Ophthalmological assessment showed bilateral complete ophthalmoplegia with mild ptosis (Fig. 1a). The muscle strength was 3/5 in the proximal muscles of upper and lower limbs and 2/5 and 3/5 in the distal muscles of lower and upper limbs respectively. He developed pectus excavatum and mild scoliosis.

Patient 2 is a 8-year old boy, the second child of a healthy probably consanguineous Ecuadorian couple originating from a small town, born at term after a pregnancy marked by polyhydramnios and decreased foetal movements. He was born at 38 weeks of gestational age by caesarean section due to foetal bradycardia with a birth weight of 3210 g and a body length of 50 cm. He presented severe hypotonia, decreased respiratory effort, facial weakness, weak cry and reduced spontaneous movements, requiring non-invasive ventilator support during the first 48 hours of life and nasogastric tube feeding

Fig. 1. Myopathic phenotype of the patients. (a, b) Clinical picture of patient 1 at the age of 34 months. (a) Due to axial muscle weakness poor posture in the upper part of the body is observed while in the sitting position. (b) Prominent protrusion of the lower ribs and minimal sunken appearance of the lower part of the sternum are noted.
(c, d) Clinical picture of patient 2 at the age of 7 years. (c) Facial weakness is present. (d) Weakness is predominant in lower limbs and lower girdle.

until day 13. Development of gross motor skills was delayed; head control was reached at 18 months and unsupported sitting at 30 months. He walked with assistance at 3 years, but independent walking was achieved only at 4 years. Consecutive serum CK levels were in normal range, and electrophysiological examinations showed normal nerve conduction velocities in upper and lower limbs with a myopathic pattern in deltoid and biceps brachii muscles on needle EMG. A muscle biopsy performed at the age of 18 months revealed a centronuclear myopathy (Fig. 2d–f). Transthoracic echocardiography showed a dilated cardiomyopathy with left ventricular ejection fraction (LVEF) of 31%, requiring treatment with digoxin and furosemide. A previous cardiologic examination, at 7 months of age, disclosed an isolated mild mitral insufficiency. The last cardiologic assessment at 7 years old showed increased dysfunction of the left ventricular ejection fraction; hence enalapril was added to the treatment. Examination at the age of 7 years revealed waddling gait, bilateral foot drop, generalized proximal weakness, more pronounced at the pelvic girdle, and he was unable to stand up from the ground without leaning to any furniture nearby. Currently, he has facial weakness; normal eye movements, high arched palate, nasal speech and globally decreased deep tendon reflexes (Fig. 1c, d). He has normal cognitive skills, and he is attending age appropriate regular school classes.

3.2. Muscle biopsy findings

Patient 1 (P1) who underwent a muscle biopsy at 13 months showed features compatible with CNM (Fig. 2a–c). It revealed increased number of fibres with central nuclei, and with NADH-TR peripheral subsarcolemmal halos and central dense areas were observed (Fig. 2a, b). There was a marked variation in fibre diameter (Fig. 2a, b). Most fibres immunolabelled with slow myosin were smaller in diameter, while the larger ones were generally fast myosin expressing (Fig. 2c), suggestive of a type 1 predominance. A few fibres showed neonatal myosin. All the other immunohistochemical analysis showed no abnormalities.

Patient 2 (P2) had a right lateral vastus muscle biopsy performed at the age of 18 months, which showed histopathological features of myotubular CNM. On haematoxylin & eosin (H&E) stain we observed the presence of abundant small rounded muscle fibres with centrally located nuclei (Fig. 2d); at NADH-TR stain subsarcolemmal peripheral halos and central dense areas were observed (Fig. 2e). Moreover scattered large whorled fibres were also noticed in COXc staining (Fig. 2f).

3.3. Whole body magnetic resonance imaging (MRI) of muscle

For patient 2, the whole body muscle resonance imaging was performed as described in the Materials and methods section at the age of 7 years. The most severely affected regions were the thighs and lower legs. No significant asymmetry in muscle involvement was observed (Supplementary Fig. S2a). Anterior compartment was more severely affected than the posterior compartment at the thigh level. Temporalis was the most affected muscle in the masticatory region with severe volume reduction. The lateral pterygoid muscles were also severely affected with relative preservation of remaining muscles. The paraspinal muscles showed a progressive increase on fat fraction, from the cervical to the lumbar region (Fig. 3 and Supplementary Fig. S2b).

Details of muscle involvement at thigh and leg levels are shown on Supplementary Fig. S2c and d. Remarkably, the rectus femoris showed a selective fat replacement, with normal signal in fibres around the tendon, which appeared opposite to the “notch” profile that has been previously described in Bethlem myopathy [10].

The anterior and posterior tibialis, and the extensor digitorum longus muscles, had the same fatty replacement pattern as rectus femoris, with preserved fibres closer to the tendon.

3.4. Genetic results

Patient 1 was sequenced and analysed for the Mendeliome gene panel as described earlier [9]. Sequencing data were filtered for rare (minor allele frequency >0.1%) variants under a recessive

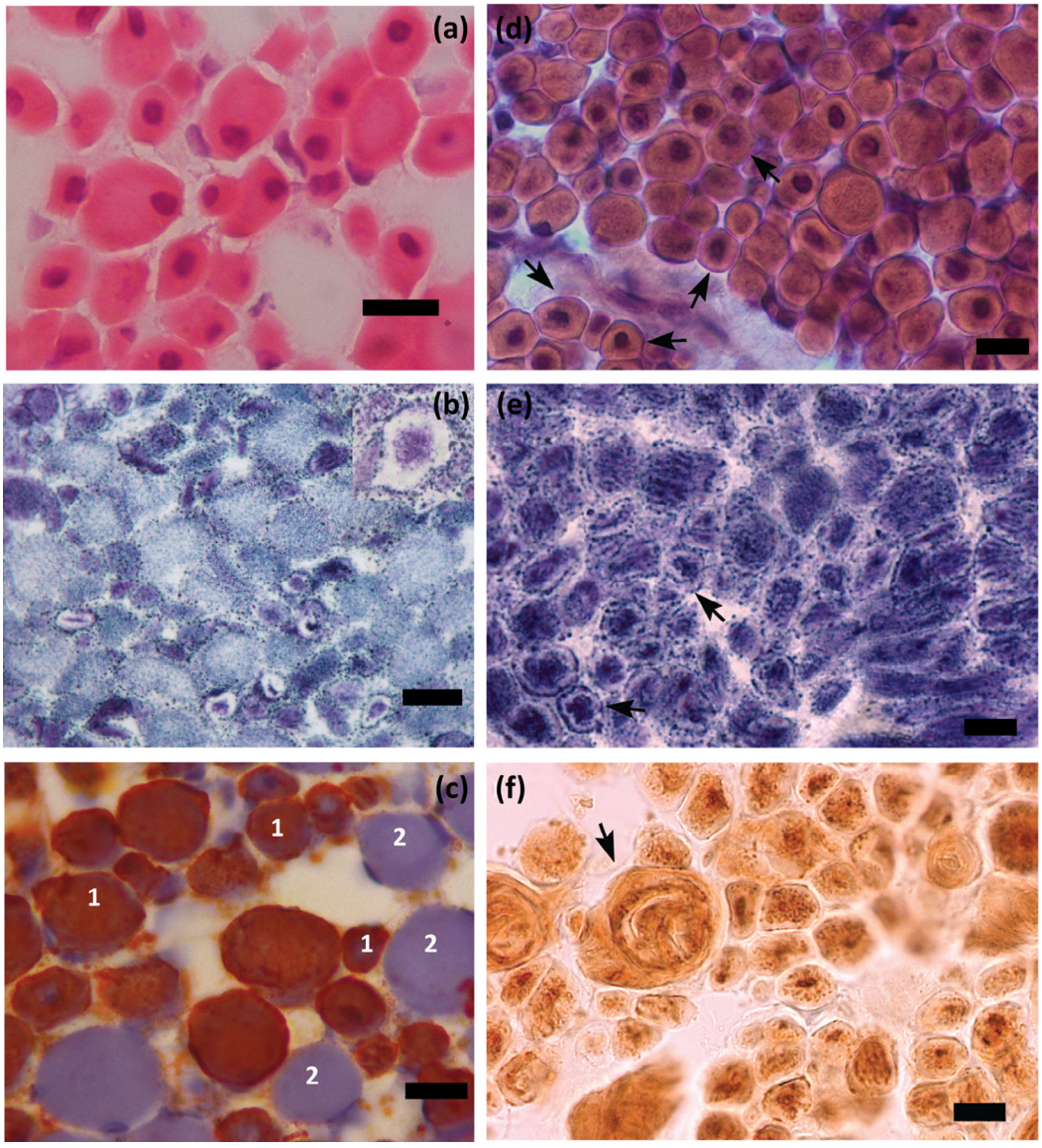

Fig. 2. Histopathological examination of patients' muscle biopsies. (a–c) Left quadriceps muscle biopsy of patient 1 at the age of 13 months. (a) The muscle biopsy showed increased fibre size variability with numerous central nuclei. H&E ×200. (b) Subsarcolemmal peripheral halos and central dense areas. NADH-TR ×400. (c) Type I fibre predominance and the most of the small fibres (including hypotrophic fibres) stained with slow myosin which are marked with '1', and fibres expressing fast myosin are marked with '2'. Slow myosin ×200. Scale bar 10 μm. (d–f) Right quadriceps muscle biopsy of patient 2 at the age of 18 months. (d) H&E stain showing numerous fibres with central nuclei (arrows) ×400. (e) NADH-TR stain. The arrows indicate fibres with the typical peripheral halo and central dense areas ×400 and (f) COXc stain showing whorled fibres (arrow) ×400. Scale bar 10 μm.

inheritance model. Six homozygous variants fitted the filter criteria (see Supplementary Table S1) and further prioritization of variants leads to the identification of a novel homozygous frameshifting mutation in *striated muscle preferentially expressed protein kinase* (*SPEG*, NM_005876, c.1626_1627insA, Thr544Aspfs*48) that was neither found in ExAC (http://exac.broadinstitute.org/) nor 1000G and introduces a premature stop codon that terminates the protein at amino acid position 591. The variant was confirmed by Sanger sequencing. Both parents were heterozygous (Supplementary Fig. S1a).

For patient 2, the targeted next-generation sequencing panel for congenital myopathy revealed a novel homozygous c.9586C>T (p.Arg3196*) *SPEG* mutation in exon 40 (further details in the Supplementary material). The mutation was confirmed by Sanger sequencing (Supplementary Fig. S1b). The novel nonsense mutation was verified to be heterozygous in the mother while the father was not available for analysis. The novel truncating mutation is reported in ExAC database only once in heterozygote state (minor allele frequency 0.000008) and affects the C-terminal Protein kinase domain of SPEG (Fig. 4).

4. Discussion

The first three myopathy patients associated with *SPEG* mutations were reported by Agrawal and collaborators [6]: 1) a severely hypotonic deceased female newborn (Agrawal P1 patient) with a homozygous nonsense mutation (c.6697C>T, p.Gln2233*) in exon 30 of *SPEG*; 2) a 6 year-old female (Agrawal P2 patient) with ophthalmoplegia, cardiomyopathy

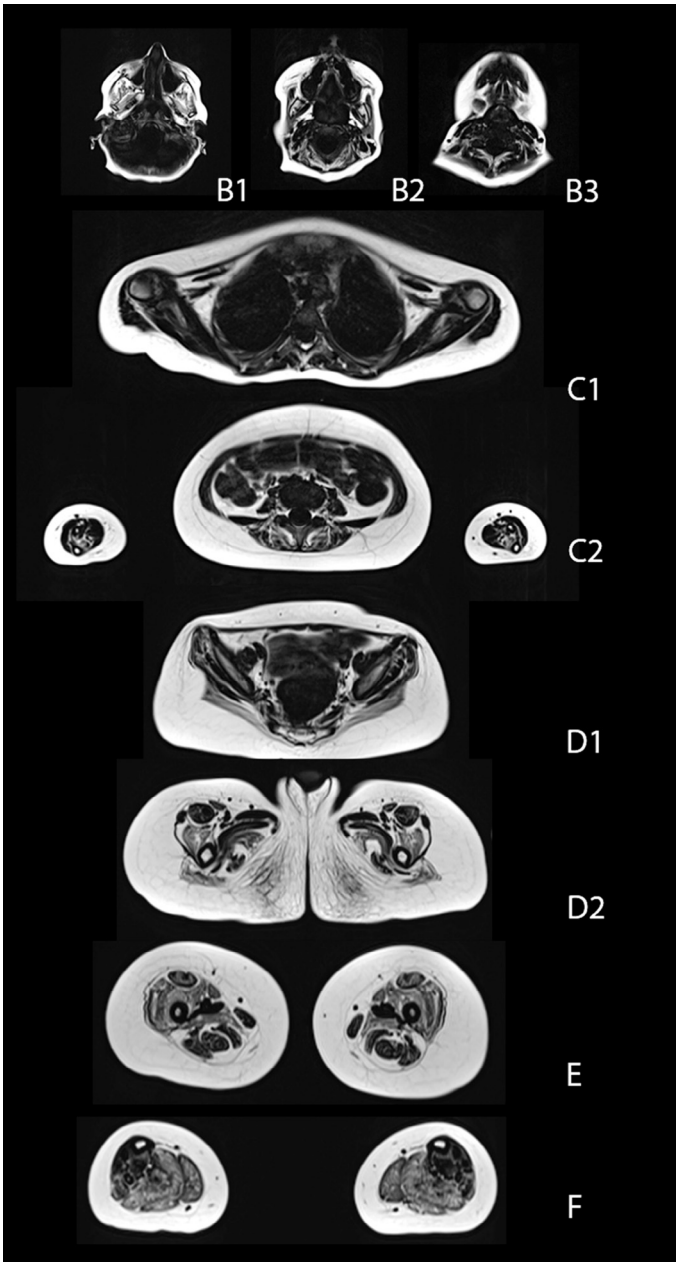

Fig. 3. Whole body MRI of the assessed muscles. Axial T1-weighted Dixon Fat-only images of the different regions of the body from top to bottom: head, neck, shoulder girdle, trunk and forearms, pelvic girdle, tight, and legs (see also Supplementary Fig. S2b for corresponding scanning positions and order).

and ventilatory support via tracheostomy but proximal muscle weakness with the ability to walk, carrying compound heterozygous mutations, a frameshift (exon 13, c.3709_3715+29del36, p.Thr1237Serfs*46) and a nonsense mutation (exon 18, c.4276C>T, p.Arg1426*); 3) a 19 month-old severely hypotonic male (Agrawal P3 patient) with dilated cardiomyopathy harbouring compound heterozygous mutation, a frameshift variant (exon 10, c.2915_2916delCCinsA, p.Ala972Aspfs*79) and a missense mutation (exon 35, c.8270G>T, p.Gly2757Val) (Fig. 4).

Here we present a second report on *SPEG* mutations: one 3 year-old boy with the typical features of a congenital myopathy and ophthalmoplegia, facial and muscle weakness who was unable to walk independently (P1) harbouring a biallelic homozygous frameshift mutation (c.1626_1627insA, Thr544Aspfs*48), and a 7 year-old boy (P2) with mild proximal muscle weakness and dilated cardiomyopathy, carrying a homozygous stop mutation (c.9586C>T, p.Arg3196*).

The human SPEG protein contains 3267 amino acids, and the SPEG complex locus appears to encode 4 isoforms that were identified in murine models: SPEGα, SPEGβ, aortic preferentially expressed gene-1 (APEG-1) and brain preferentially expressed gene (BPEG) [11,12]. Both SPEGα and SPEGβ are highly expressed in striated muscle and cardiomyocytes in early periods of life during maturation. The region in the C-terminal (amino acid 2530–2674) including the last Ig-like domain and fibronectin III domain is required for interaction with MTM1. Among the current reported cases, Agrawal-P1 patient with a nonsense mutation predicting a truncated SPEG protein p.Gln2233* manifested the most severe phenotype as the patient deceased in the neonatal period, which could be explained by the loss of the C-terminal interaction region with MTM1 or the absence of protein expression although no proof was so far documented due to lack of material. Agrawal-P2 and -P3 both showed dramatic reduced protein expression levels of SPEGα and SPEGβ. It appeared that skeletal muscle weakness, early onset dilative cardiomyopathy and eye muscle weakness were the main pathological manifestations. The differential involvement of the skeletal muscle, myocardium and the external eye muscles needs to be distinguished and differentiated when interpreting genotype–phenotype correlations. Agrawal-P2 patient was more severe than Agrawal-P3 since Agrawal-P2 had ophthalmoplegia, dilated cardiomyopathy and significant skeletal muscle weakness, including respiratory and swallowing difficulties. Although Agrawal P3 was very young, ophthalmoplegia and cardiomyopathy were not reported. The expression of the mutant SPEG allele p.Gly2757Val in Agrawal-P3 patient might be partially functional and may prevent a cardiomyopathy since the single amino acid change occurred beyond the interaction region with MTM1.

The novel mutation in our P2 is predicted to result in a truncated C-terminal SPEGβ p.Arg3196* with loss of a small portion of the second kinase domain, but without affecting the MTM1 interaction region. Clinico-pathologically the severity of this patient shows the same pattern as Agrawal-P3, since both patients have moderate proximal weakness and dilated cardiomyopathy with no need of assisted ventilation (Table 1). Moreover, P2 has the mildest skeletal muscle phenotype of the known SPEG mutations so far described. The interpretation here is that mutations did not disrupt the MTM1 interaction region of SPEG in both patients. Since our patient P2 did not develop eye muscle involvement it is likely that the truncated C-terminal kinase domain of SPEG might not be essential for eye muscle function, but experimental studies are required to confirm this hypothesis.

Remarkably, our patient P1 (Table 1) displayed a congenital myopathy phenotype with moderate hypotonia, absence of cardiomyopathy and without requiring assisted ventilation or tracheostomy. The mutation in P1 results in an N-terminal frameshift truncated protein ending before the Ig-like domain2 (Fig. 4), also involving the C-terminal interaction domain of

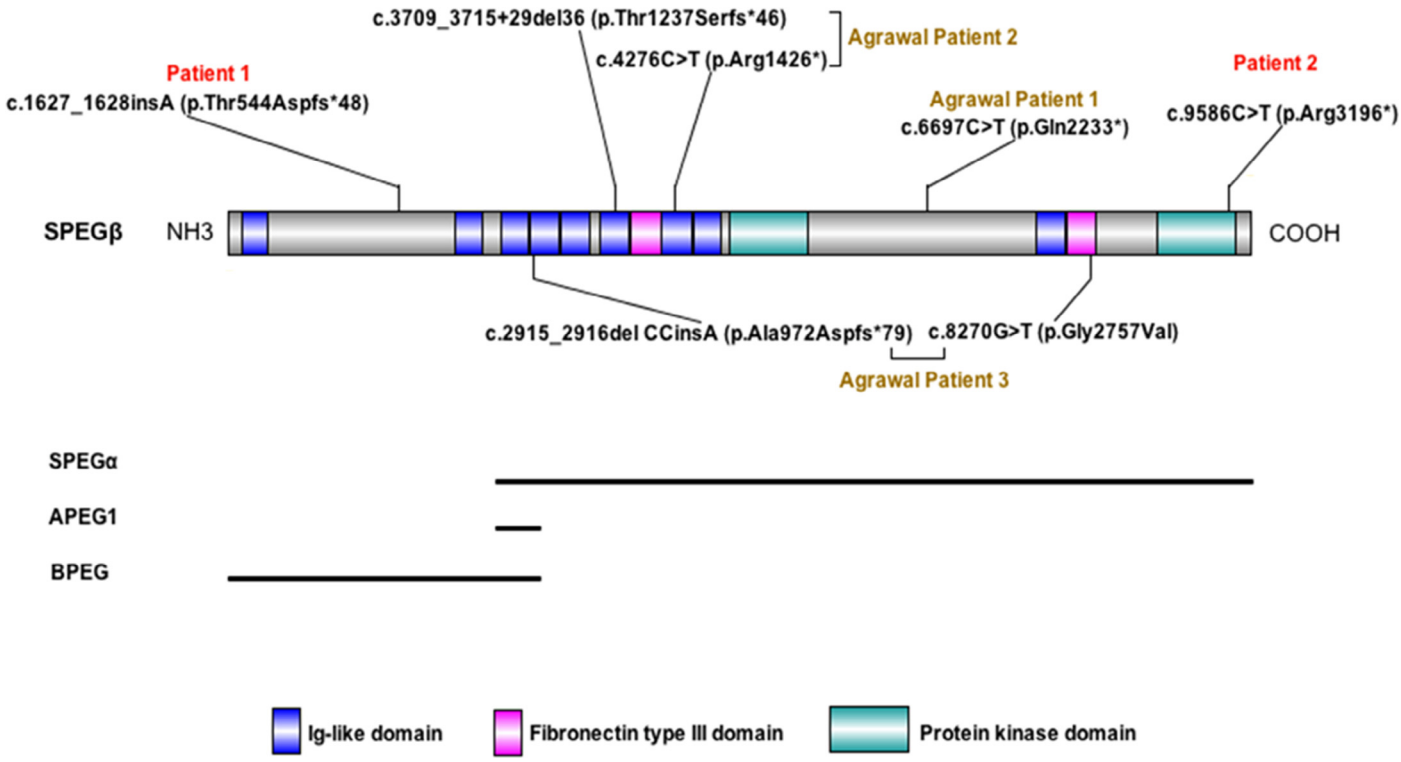

Fig. 4. SPEG domain organization and disease causing mutations. Schematic representation of SPEG protein domains and position of the mutations identified so far, generated by Illustrator for Biological Sequences: IBS. In red (Patients 1 and 2) are reported two new cases with novel mutations identified in our study, other previous reported cases are labelled as Agrawal Patients 1, 2, 3. The longest variant of human SPEG corresponds to the murine SPEG β; other known murine SPEG variants are illustrated below as thick straight black lines.
Abbreviations: Ig, Immunoglobulin; Fb, fibronectin; PK, protein kinase.

Table 1
Molecular and clinicopathological findings in individuals carrying *SPEG* mutations.

	P1	P2
Sex	Male	Male
Current age	3 years	7 years
SPEG exons	exon 4	exon 40
Mutation	c.1627-1628insA, p.Thr544Aspfs*48	c.9586C>T, p.Arg3196*
Clinical phenotype	Full-term caesarean section due to foetal bradycardia	Poor foetal movements, 38 weeks of gestational age by caesarean section due to foetal bradycardia
	At day 5 NICU with apnoea, poor sucking and high-pitched cry, but no need of intubation	Decreased respiratory effort, weak cry, non-invasive ventilator support in first 48 hours of life
	Head control at 6 months, sitting unsupported with 12 months; but unable to walk independently so far	Head control at 18 months, sitting position at 30 months, assisted walking at 3 years, independent walking at 4 years
	Pectus excavatum;	Generalized mild proximal weakness and independent ambulation
	Recurrent pulmonary infections; no cardiomyopathy so far	Reduced left ventricular ejection fraction 31% and requiring digoxin and furosemide, recently with addition of enalapril;
	Facial weakness, ptosis, ophthalmoplegia	Facial weakness, normal eye movements
Biopsy findings	Central nuclei, some peripheral nuclei	Abundant small rounded muscle fibres, central nuclei
	increased fibre size variability, type 1 fibre predominance and hypotrophy, clear halos and central dense areas on NADH-TR	Increased fibre size variability, large whorled-like fibres, NADH-TR stain subsarcolemmal peripheral halos and central dense areas

SPEGβ with MTM1. Thus the absence of cardiomyopathy is surprising although it is predicted to result in a myopathy and cardiomyopathy at the same range of severity as Agrawal-P2 [7]. A possible mechanism to explain the lack of cardiomyopathy in P1 could be that single nucleotide insertion in *SPEG* (c.1627_1628insA) in P1 might have an impact on transcriptional regulation of SPEG isoforms. The SPEG complex gene locus is expressing multiple isoforms (data from GTEx Portal http://www.gtexportal.org/), and some correspond to the four main isoforms identified in mouse. A previous study [11] in mouse suggested that the transcription of SPEGα is initiated from a promoter, which is located downstream of the promoter for transcription of SPEGβ; thus SPEGα is an N-terminal truncated form of SPEGβ. The P1 *SPEG* mutation (c.1627_1628insA, p. Thr544Aspfs*48) is the only one among all the five known disease related variants that does not introduce

mutations to SPEGα (Fig. 4); it affects only SPEGβ. Besides, SPEGα and SPEGβ are both reported to be regulatory proteins within the junctional membrane complex (JMCs) that regulates junctophilin-2 (JPH2) phosphorylation, which is important for transverse tubules maintenance in cardiac myocytes. Thus we could speculate that in P1 the functional SPEGα might partially compensate the loss of SPEGβ and rescue partially the pathology in P1. So far it is known that in skeletal muscle, SPEG interacts with Myotubularin, and also colocalizes with dihydropyridine receptor (DHPR), sarcoplasmic reticulum Ca^{2+} ATPase (SERCA),;thus it plays an essential role in the differentiation of muscle cells, in excitation contraction coupling, and also in controlling intermediate filament architecture and muscle maintenance. SEPG is also essential for cardiac function as SPEG regulates two key components in the junctional membrane complexes (JMCs), the cardiac Ca^{2+} release channels ryanodine receptors (RYR2) and JPH2. However, only the N-terminal domain of SPEGβ is able to interact with RYR2 for Ca^{2+} release in SR in cardiac myocytes [7]. Reduction or loss of SPEG impairs JPH2 phosphorylation, which leads to disruption of T-tubules and hyperactivation of RYR2, eventually may be the mechanism leading to heart failure.

The MRI findings on our patient differ in some aspects from those reported on MTM1 related myotubular myopathy. At the thigh level there is a predominant alteration of the anterior compartment instead of the posterior compartment described on MTM1 patients but at the lower leg level the predominance of posterior leg muscle compromise and relatively sparing of anterior tibial muscle are findings similar to those in MTM1 patients. Moreover, relative preservation of the adductor longus and gracilis with severe involvement of the adductor magnus [13] also shows similarities with MTM1. Comparable to DNM2 centronuclear myopathy, SPEG related congenital myopathy shows a relative preservation of the rectus femoris and gracilis at the thigh level, but in DNM2 patients there is an early involvement of tibial anterior muscle not seen in our patient [14].

Histologically SPEG muscle biopsies represent a challenge for the pathologist. The histological pattern is remarkably similar to other forms of CNM consisting of central nuclei, clear peripheral halos and central dense areas on NADH-TR, as well as type 1 fibre predominance and hypotrophy fits to the other described forms of CNM myopathies (i.e. *MTM1*, *DNM2*). We did not observed typical necklace fibres or radiating strands on NADH-TR staining in the biopsies of our patient. However, fibres with a peripheral halo have been observed. Whether older patients may present with necklace fibres or other features resembling different forms of CNM as initially suggested remains to be elucidated in larger studies. This fact enhances the need for thorough clinical phenotyping as in Patient 2 reported here, in whom the cardiomyopathy was the key finding that led to the correct diagnosis, since other forms of centronuclear myopathies do not affect cardiac function. Ultimately, identification of additional patients is needed before more insights on genotype–phenotype correlations can be obtained as the clinical variability might also be due to additional genetic polymorphisms, in particular in SPEG interacting partners or within the E-C coupling axis.

Acknowledgements

Our patients and their parents are gratefully acknowledged. This work was supported by Muscular Dystrophy Association (255889), USA, and Deutsche Forschungsgemeinschaft (CI 218/1-1), Germany grants to Dr. Sebahattin Cirak. Clínica Las Condes, Santiago, Chile: PIDA. 2014-002, grants to Dr. Claudia Castiglioni, Ministry of Health Grant Finalizzata 201201X002951 and Telethon GUP13004 grants to Fabiana Fattori and Enrico Bertini and Grant FONDECYT 1151383 to Jorge Bevilacqua.

We are grateful to the Cologne Center for Genomics for performing the next generation sequencing.

Appendix: Supplementary material

Supplementary data to this article can be found online at doi:10.1016/j.nmd.2017.05.014.

References

[1] Nance JR, Dowling JJ, Gibbs EM, Bönnemann CG. Congenital myopathies: an update. Curr Neurol Neurosci Rep 2012;12:165–74.
[2] Romero NB. Centronuclear myopathies: a widening concept. Neuromuscul Disord 2010;20:223–8.
[3] Laporte J, Hu LJ, Kretz C, Mandel JL, Kioschis P, Coy JF, et al. A gene mutated in X-linked myotubular myopathy defines a new putative tyrosine phosphatase family conserved in yeast. Nat Genet 1996;13:175–82.
[4] Böhm J, Biancalana V, Malfatti E, Dondaine N, Koch C, Vasli N, et al. Adult-onset autosomal dominant centronuclear myopathy due to BIN1 mutations. Brain 2014;137:3160–70.
[5] Ceyhan-Birsoy O, Agrawal PB, Hidalgo C, Schmitz-Abe K, DeChene ET, Swanson LC, et al. Recessive truncating titin gene, TTN, mutations presenting as centronuclear myopathy. Neurology 2013;81:1205–14.
[6] Agrawal PB, Pierson CR, Joshi M, Liu X, Ravenscroft G, Moghadaszadeh B, et al. SPEG interacts with myotubularin, and its deficiency causes centronuclear myopathy with dilated cardiomyopathy. Am J Hum Genet 2014;95:218–26.
[7] Quick AP, Wang Q, Philippen LE, Barreto-Torres G, Chiang DY, Beavers D, et al. SPEG (Striated Muscle Preferentially Expressed Protein Kinase) is essential for cardiac function by regulating junctional membrane complex activity. Circ Res 2017;120:110–19.
[8] Dubowitz V, Sewry CA, Oldfors A. Muscle biopsy: a practical approach. 4th ed. 2013.
[9] Kawalia A, Motameny S, Wonczak S, Thiele H, Nieroda L, Jabbari K, et al. Leveraging the power of high performance computing for next generation sequencing data analysis: tricks and twists from a high throughput exome workflow. PLoS ONE 2015;10:e0126321.
[10] Mercuri E, Lampe A, Allsop J, Knight R, Pane M, Kinali M, et al. Muscle MRI in Ullrich congenital muscular dystrophy and Bethlem myopathy. Neuromuscul Disord 2005;15:303–10.
[11] Hsieh CM, Fukumoto S, Layne MD, Maemura K, Charles H, Patel A, et al. Striated muscle preferentially expressed genes α and β are two serine/threonine protein kinases derived from the same gene as the aortic preferentially expressed gene-1. J Biol Chem 2000;275:36966–73.
[12] Hsieh CM, Yoshizumi M, Endege WO, Kho CJ, Jain MK, Kashiki S, et al. APEG-1, a novel gene preferentially expressed in aortic smooth muscle cells, is down-regulated by vascular injury. J Biol Chem1996;271:17354–9.
[13] Bevilacqua JA, Bitoun M, Biancalana V, Oldfors A, Stoltenburg G, Claeys KG, et al. "Necklace" fibers, a new histological marker of late-onset MTM1-related centronuclear myopathy. Acta Neuropathol 2009;117:283–91.
[14] Catteruccia M, Fattori F, Codemo V, Ruggiero L, Maggi L, Tasca G, et al. Centronuclear myopathy related to dynamin 2 mutations: clinical, morphological, muscle imaging and genetic features of an Italian cohort. Neuromuscul Disord 2013;23:229–38.